SCIENCE CHINA
Life Sciences

• RESEARCH PAPER •

March 2012 Vol.55 No.3: 228–235
doi: 10.1007/s11427-012-4296-9

RAB-27 and its effector RBF-1 regulate the tethering and docking steps of DCV exocytosis in *C. elegans*

FENG WanJuan[1†], LIANG Tao[1†], YU JunWei[1†], ZHOU Wei[1], ZHANG YongDeng[1], WU ZhengXing[1] & XU Tao[1,2*]

[1]*College of Life Science and Technology, Huazhong University of Science and Technology, Wuhan 430074, China;*
[2]*National Laboratory of Biomacromolecules, Institute of Biophysics, Chinese Academy of Sciences, Beijing 100101, China*

Received August 24, 2011; accepted January 18, 2012

The molecular mechanisms by which dense core vesicles (DCVs) translocate, tether, dock and prime are poorly understood. In this study, *Caenorhabditis elegans* was used as a model organism to study the function of Rab proteins and their effectors in DCV exocytosis. RAB-27/AEX-6, but not RAB-3, was found to be required for peptide release from neurons. By analyzing the movement of DCVs approaching the plasma membrane using total internal reflection fluorescence microscopy, we demonstrated that RAB-27/AEX-6 is involved in the tethering of DCVs and that its effector rabphilin/RBF-1 is required for the initial tethering and subsequent stabilization by docking.

exocytosis, dense core vesicles, RAB-3, RAB-27, *C. elegans*, total internal reflection fluorescence microscopy

Citation: Feng W J, Liang T, Yu J W, *et al*. RAB-27 and its effector RBF-1 regulate the tethering and docking steps of DCV exocytosis in *C. elegans*. Sci China Life Sci, 2012, 55: 228−235, doi: 10.1007/s11427-012-4296-9

Rab GTPases constitute the largest family of small GTPases that function as molecular switches that alternate between two conformational states: the GTP-bound active form and the GDP-bound inactive form. Rab proteins are reversibly associated with organelle membranes, a feature inherent to their role as regulators of membrane trafficking. Through the recruitment of various effector proteins, Rab proteins serve as multifaceted organizers of virtually all membrane trafficking processes, ranging from vesicle budding, uncoating, motility and tethering to docking and fusion [1–3].

Certain Rab GTPases, such as Rab3 and Rab27, referred to as secretory Rabs, mediate various types of regulated exocytic events [4,5]. In both *C. elegans* and mice, the knockout of *rab3* genes causes only mild defects in synaptic transmission [6,7], which suggests the existence of functional redundancy with other Rabs in the release of synaptic vesicles (SVs). In support of these observations is recent work that has shown that both Rab3 and Rab27 are required for synaptic transmission in *C. elegans* [5].

Besides SVs, another important type of secretory vesicles is the so-called dense core vesicles (DCVs) in which secretory proteins, specifically neuropeptides and peptide hormones, are stored. DCVs are thought to have evolved to meet the need for storage and acute release of large amounts of proteins on demand. DCVs and SVs are apparently distinct organelles responsible for different types of neurosecretion. Thus, these two classes of secretory organelles may use different sets of molecules in exocytosis. It is not clear whether DCVs use different or similar sets of Rab proteins as SVs for coordinating exocytosis. There are two isoforms of Rab27 (Rab27A and Rab27B) in mammals, whereas there is only one isoform (AEX-6) in *C. elegans*. Lesions in both Rab27A and Rab27B genes in mice have recently

† Contributed equally to this work
*Corresponding author (email: xutao@ibp.ac.cn)

suggested an indispensible role for Rab27 in the docking of DCVs [8,9]. The role of Rab3 in DCV exocytosis remains controversial. Data from bovine adrenal chromaffin cells, showed that Rab3 genes overexpression in wild-type or mutant Rab3 paralogs decreased secretion [10,11]. There are four paralogs of Rab3 (Rab3A, Rab3B, Rab3C, Rab3D) in mammals, which makes it challenging to study the individual roles of Rab3s and their effectors in DCV exocytosis. In a recent study of quadruple Rab3 knockout mice, the authors proposed that Rab3 may be involved in both DCV biogenesis and priming [12]. *C. elegans* expresses only one *rab-3* gene, which makes it an ideal organism for the study of Rab3 function in DCV exocytosis.

The GTP membrane-bound form of Rab proteins typically binds to a variety of effectors that regulate particular steps of membrane transport and cell signaling [1,13]. Rabphilin (known as RBF-1 in *C. elegans*) is a putative effector of Rab3 and Rab27 [14–16]. Vertebrate Rab3 and Rab27 both bind to rabphilin via a zinc-finger Rab-binding domain [16]. In contrast, *C. elegans* rabphilin/RBF-1 interacts only with RAB-27/AEX-6, but not with RAB-3 [17]. The mechanism that describes how rabphilin cooperates with Rab proteins in DCV tethering and docking is poorly understood.

In the current study, we used *C. elegans* as a model organism to study the requirement of Rabs and their effectors for DCV exocytosis. We quantified neuropeptide release by monitoring the uptake of GFP-tagged neuropeptides into coelomocytes *in vivo*. In addition, we used total internal reflection fluorescence microscopy (TIRFM) to track the movements of single DCVs approaching the plasma membrane. Through a combination of these methods, we found that RAB-27/AEX-6 and its effector rabphilin/RBF-1 are required for DCV exocytosis at different steps, whereas RAB-3 is dispensable for DCV secretion.

1 Materials and methods

1.1 *C. elegans* strains

Nematode strains were maintained at 20°C by standard methods [18,19]. The strains used in this study were as follows: *aex-6(sa24)*, *rab-3(js49)*, *unc-18(e81)*, *rbf-1(js232)*, *ida-1::gfp* KM246 and *anf::gfp* EG3680 [20]. We crossed *aex-6(sa24)* with *rbf-1(js232)*. KM246 and EG3680 were crossed with all four strains, *aex-6(sa24)*, *rab-3(js49)*, *rbf-1(js232) and unc-18 (e81)*.

1.2 Embryonic cell cultures

Embryonic cells were isolated from nematode eggs and cultured as described [21,22]. The cells were plated on peanut lectin (0.5 mg mL^{-1}, Sigma)-coated cover-glasses and maintained in L-15 medium. The cells were incubated at 20°C in a humidified incubator. The culture medium was adjusted to 340 mOsm with sucrose and filter-sterilized. Cells that were cultured for 3–4 days were used in the experiments.

1.3 ANF-GFP release assay

The ectopically expressed neuropeptide ANF-GFP (GFP-tagged atrial natriuretic factor) was measured as the intensity of fluorescence in coelomocytes, as previously described [20]. The imaging of immobilized worms was performed on an Andor Revolution XD laser confocal microscope system based on spinning-disc confocal scanning (Yokogawa Electric Corporation) under the control of the Andor IQ 1.91 software. Microscope images were taken on an Olympus IX-71 inverted microscope (Olympus, Japan) with a 60× objective lens (NA=1.45, Olympus, Japan). Only the coelomocytes that were not masked by other tissues (gut and gonads) and did not abut against the body wall were captured. The total pixel intensity in wild-type worms was set to an arbitrary fluorescence unit (A.U.) of 1.0 to enable comparison with other strains. Images were displayed and analyzed by ImageJ 1.43b (Wayne Rasband, USA).

1.4 TIRFM imaging

Our TIRFM setup was constructed as previously described [23]. A 488 nm laser was used for fluorescence excitation. Images were acquired at 40 Hz with a 25 ms exposure by $iXon^{EM}$+885 EMCCD (Andor Technology, UK) with a pixel size of 80 nm. We calculated the penetration depth of the evanescent field (d=109 nm) by measuring the incidence angle with a prism (n=1.516) and a 488 nm laser beam. Imaging was controlled by the Andor IQ 1.91 software. The stacks of TIRF images were analyzed with a self-written Matlab program (Mathworks, Natick, MA, USA). Single vesicle detection was performed using à trous wavelet transformation, with the level k=3 and the detection level ld=1.0 [24], to produce a binary mask image. Only spots with areas larger than 4 (2×2) pixels were accepted as vesicles for further analysis. The fluorescence intensity and positions of the vesicles were determined using a 2D Gaussian fitting with an offset background. For tracking vesicles, we used a robust single particle tracking algorithm provided by Khuloud Jaqaman [25].

1.5 Statistics

All data were presented as the mean±standard error of the mean (SEM) with the indicated number of experiments. Statistical significance was evaluated by Student's t test or the Mann-Whitney rank sum test according to the normality of the data distribution in SigmaStat 3.11 (Systat Software, Inc). A significant difference is indicated by asterisks (*, P<0.05; **, P<0.01; ***, P<0.001). All comparisons were made between paired experiments that were performed on

the same day and under the same conditions.

2 Results

2.1 RAB-27 but not RAB-3 is required for the release of ectopically expressed peptides in neurons

To directly assess the role of RAB-27/AEX-6 in DCV exocytosis, we measured the ANF-GFP fluorescence intensity in the coelomocytes of *C. elegans*. ANF-GFP was ectopically expressed throughout the nervous system driven by a pan-neuronal *aex-3* promoter. ANF-GFP has been demonstrated to be packaged into DCVs and is released into the pseudocoelom, which is then absorbed by scavenging coelomocyte cells [20]. The GFP fluorescence intensity of coelomocytes in *aex-6(sa24)* mutants was significantly reduced compared with the wild-type strain (64% reduction) (Figure 1A and B). As a positive control, we examined UNC-18, which had been proposed to be absolutely necessary for vesicle docking and fusion [26,27]. In *unc-18(e81)* mutants, the fluorescence intensity in coelomocytes was reduced to a similar level as that in *aex-6(sa24)* mutants (Figure 1B). It is unclear where the remaining fluorescence came from because the *unc-18* null mutation should block all regulated exocytoses [28,29]. It is plausible that a portion of the peptides may be sorted into the constitutive secretory pathway, which is UNC-18-independent [30]. Nevertheless, the observation that in *aex-6* mutants neuropeptide release was blocked to a similar extent as it was in *unc-18* mutants suggests that RAB-27/AEX-6 is necessary for DCV exocytosis.

A recent study in *C. elegans* has indicated that both RAB-3 and RAB-27 are involved in the exocytosis of SVs [5]. We then investigated whether this was also true for DCV exocytosis. Interestingly, we observed no significant change in the fluorescence intensity of ANF-GFP in the coelomocytes of *rab-3(js49)* mutants (Figure 1B). In addition, we confirmed that the density and the dwelling rate of DCVs in the TIRF zone underneath the plasma membrane were changed in *rab-3(js49)* mutants (Appendix Figure 1). Taken together, our data suggest that RAB-3 is not required for DCV exocytosis in *C. elegans*.

2.2 RBF-1 mutants exhibit reduced levels of ANF-GFP fluorescence in coelomocytes

Rab proteins regulate vesicle traffic through interactions with distinct effectors [1]. We further studied the level of ANF-GFP fluorescence in the RAB-27 effector, rabphilin/RBF-1. The ANF-GFP fluorescence was reduced (~40%) in *rbf-1(js232)* mutants, which indicated the involvement of RBF-1 in DCV exocytosis. Double mutants of *aex-6(sa24)* and *rbf-1(js232)* produced greater reduction than did the *aex-6(sa24)* single mutants (Figure 1C), suggesting that there are non-overlapping functions of rabphilin/RBF-1 and RAB-27/AEX-6 in DCV exocytosis.

ANF-GFP was seen throughout the nervous system with fluorescence localized in the nerve ring as well as in the dorsal and ventral nerve cords (Figure 2A). The reduction of ANF-GFP fluorescence was the result of a release defect because ANF-GFP fluorescence was observed to have slightly increased rather than decreased in the dorsal nerve cords and the nerve ring region in both *aex-6* and *rbf-1* single mutants (Figure 2C). We also excluded the possibility of any influence on endocytosis in these mutants by quantifying the absorption ability of coelomocytes injected with rhodamine-conjugated dextran (10 kD) (Figure 2B and D).

2.3 Quantifying the behavior of DCVs approaching the plasma membrane using TIRFM

To further investigate the exact step(s) that RAB-27 participates in during DCV exocytosis, we used time-lapsed TIRFM to track the dynamic behavior of individual DCVs. DCVs labeled by IDA-1::GFP in *C. elegans* move faster than in mammalian cells [31]. We thus acquired TIRF images with a high sampling frequency, up to 40 Hz (25 ms per frame), and observed the movement of DCVs at a higher time resolution. Most vesicles that entered the TIRF zone within ~100 nm from the plasma membrane were not stabilized at one position. Instead, they moved rapidly either laterally or out of the TIRF zone. These vesicles were regarded as mobile vesicles that are not physically attached to the plasma membrane. We estimated that the average density of vesicles from many snapshots reflected the number of vesicles that could translocate to the plasma membrane. Of all the vesicles that appeared in the TIRF zone, a subset remained static at a given site for a defined period while maintaining a relatively constant level of fluorescence. We defined a dwelling event as the 2D displacement of a vesicle by 80 nm or less (1 pixel size of our CCD camera) for at least three consecutive frames (75 ms) (Figure 3A). Dwelling may occur because vesicles are physically tethered to the plasma membrane. The shape of the distribution of the dwelling times of DCVs was skewed, most of the data were within a short range (<0.2 s) and only a few were within a long range (Figure 3D and E). We defined those that dwelled less than 0.2 s as short-retained vesicles, which may reflect a state of tethering or unstable docking, whereas those that dwelled more than 0.2 s were classified as long-retained vesicles, which may reflect a state of stabilized docking.

We validated our quantification method with the *unc-18* mutants, which are known to affect the docking of DCVs. As expected, the vesicle densities calculated from snapshots were not significantly different between wild-type and *unc-18* animals (Figure 3B), suggesting that the translocation of DCVs into the TIRF zone was not affected by the absence of UNC-18. However, a reduction in the dwelling rate of DCVs in *unc-18* mutants was observed (Figure 3C). Both the short-retained and the long-retained vesicles were

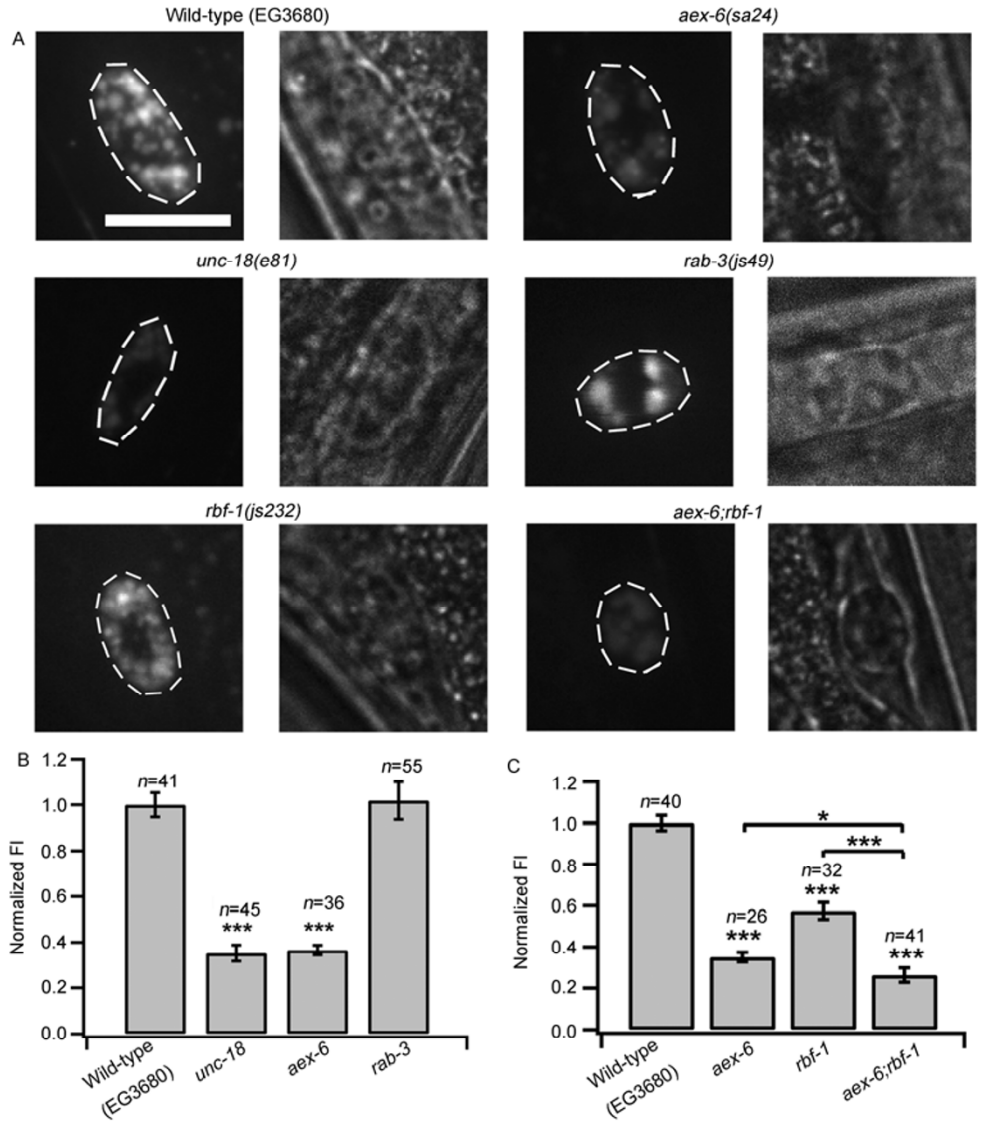

Figure 1 RAB-27/AEX-6 and its effector rabphilin/RBF-1, but not RAB-3, are required for the release of ectopically expressed ANF-GFP in neurons. A, Representative examples shown are ANF-GFP fluorescent and bright field images of coelomocytes in worms of the indicated strains. Scale bar, 10 μm. B, Histograms show the averaged total fluorescence intensity of ANF-GFP in coelomocytes in wild-type, *unc-18*, *aex-6* and *rab-3* mutant worms. C, Histograms show the average total fluorescence intensity of ANF-GFP in coelomocytes in wild-type, *aex-6*, *rbf-1* and *aex-6;rbf-1* mutant worms.

reduced, with a greater reduction for the long-retained vesicles, in *unc-18* mutants. These results are consistent with a role for UNC-18 in the tethering/docking of secretory vesicles at the plasma membrane [26,32].

2.4 RAB-27 and rabphilin act together to regulate translocation and docking of DCVs

We next set-out to understand the action site(s) of RAB-27/AEX-6 and its effector, rabphilin/RBF-1. In *aex-6* mutants, the snapshot vesicle density was not significantly different from that of the wild-type N2 worms (Figure 4A). In the RAB-27 effector RBF-1, there was no effect on vesicle density in its single mutants or in *aex-6* single mutants (Figure 4A). However, when both *aex-6* and *rbf-1* were mutated, there was a considerable reduction in vesicle density in the TIRF zone (Figure 4A), suggesting that both proteins function redundantly in the translocation of DCVs to the plasma membrane. We did observe a significant reduction in the dwelling rate of DCVs in *aex-6* mutants (Figure 4B). Interestingly, the reduction in dwelling events was mainly due to a reduced number of short-retained vesicles, whereas no statistically significant reduction in the long-retained vesicles was observed (Figure 4D). Unlike the *aex-6* mutants, both the short- and long-retained DCVs were significantly reduced in the *rbf-1* mutants (Figure 4D). The *aex-6;rbf-1* double mutants behaved similar to the *rbf-1* single mutants in the dwelling of DCVs at the plasma membrane (Figure 4D). These results suggest that rabphilin

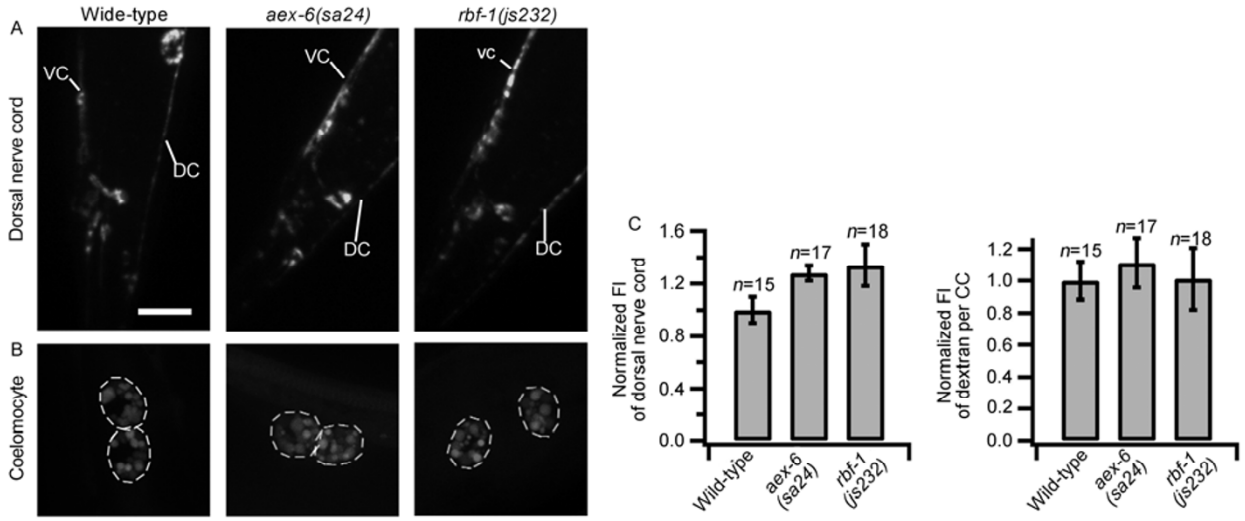

Figure 2 Decreased ANF-GFP uptake was not caused by defects in expression or endocytosis. A, Images of the EG3680[*Paex-3::ANF::GFP*] strain in the background of wild-type (WT), *aex-6* mutants and *rbf-1* mutants. VC, ventral nerve cord; DC, dorsal nerve cord. Scale bar, 10 μm. B, Dextran (10 kD) was endocytosed by coelomocytes in wild-type, *aex-6* and *rbf-1*. C, Histograms show the average total fluorescence intensity of ANF-GFP in the DC from wild-type, *aex-6* and *rbf-1* worms. D, Histograms show the averaged total fluorescence intensity of dextran (10 kD) in coelomocytes from wild-type, *aex-6* and *rbf-1* worms.

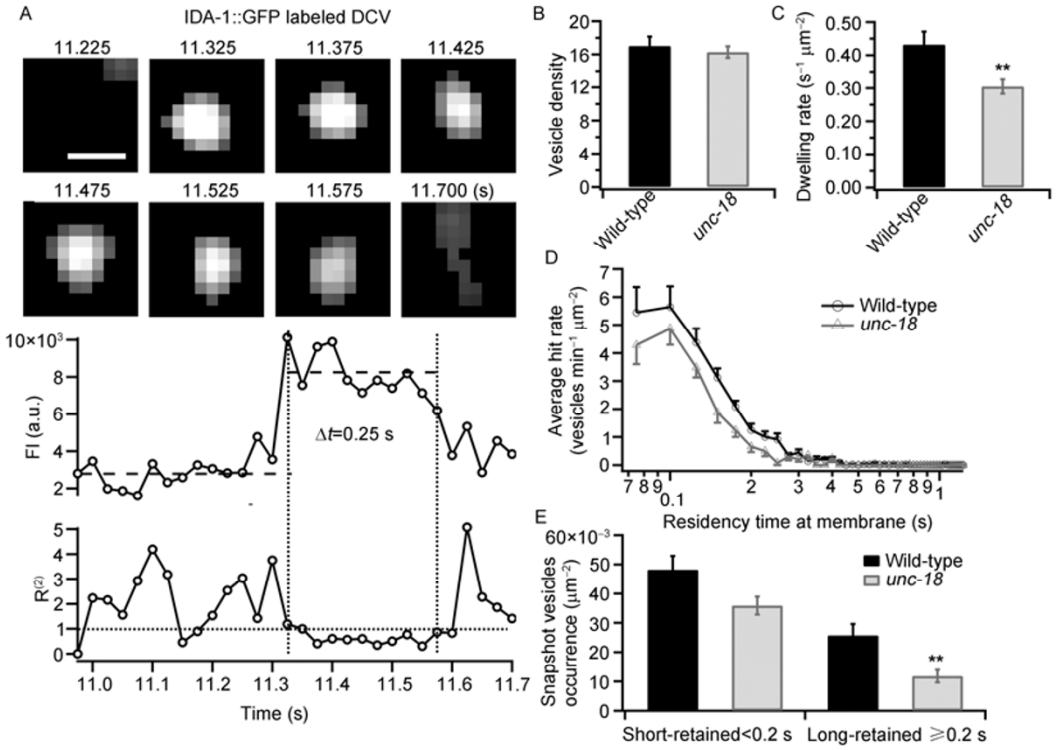

Figure 3 Quantification of the docking behavior of DCVs in the TIRF zone. A, Sequential images of a single DCV labeled with IDA-1::GFP from a live ALA neuron (upper panel) with the corresponding time course of fluorescence intensity (FI, in arbitrary unit) and the 2D displacement $R^{(2)}$. The horizontal dotted line marks the $R^{(2)}$ level of 1 pixel (80 nm), which was used as a threshold to identify immobilization. The duration of vesicular $R^{(2)}$ below this threshold combined with fluorescence intensity above the threshold (indicated by two vertical dashed lines) measured the dwell time (0.25 s in this case). Scale bar, 0.4 μm. B, Density of the total visible DCVs (m^{-2}) in the TIRF zone from wild-type (n=16) and *unc-18(e81)* (n=14) mutants. C, Dwelling rate of DCVs (per second per unit area). D, Lifetime distribution of vesicles hitting the plasma membrane. E, Average vesicle abundance at given times during image acquisition, grouped according to their residency times at the plasma membrane.

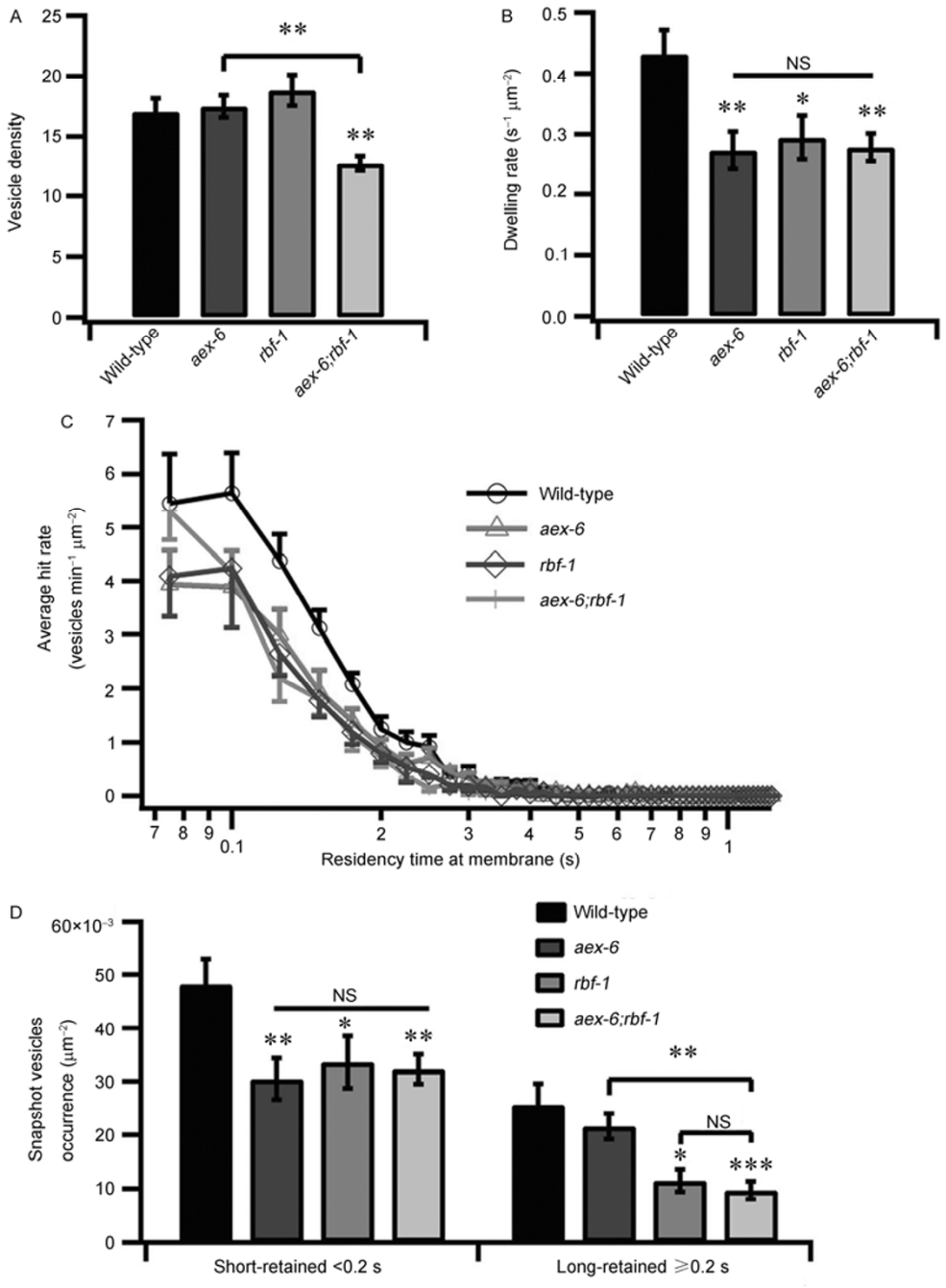

Figure 4 Rabphilin (RBF-1) participates in the stabilized docking of DCVs. A, Density of total visible DCVs (m^{-2}) in the evanescent field from wild-type (n=16) and *aex-6(sa24)* (n=15), *rbf-1(js232)* (n=13) and *aex-6(sa24);rbf-1(js232)* (n=13) double mutants. B, Dwelling rate of DCVs (per second per unit area). C, Lifetime distribution of vesicles hitting the plasma membrane. D, Average vesicle abundance at given times during image acquisition, grouped according to their membrane residency times.

is involved in stabilizing the docking of DCVs at the plasma membrane. Taken together, these data suggest that RAB-27 and rabphilin play an important role in the docking step of DCVs at the plasma membrane, possibly in the initial tethering of the vesicles. Subsequently, rabphilin/RBF-1 is further required to stabilize docking and, ultimately, makes the DCV fusion competent.

3 Discussion

As compared with synaptic vesicles, the exact roles of Rab proteins and their effectors in DCV exocytosis are not well characterized. This is partially due to the high degree of redundancy of Rabs in higher organisms. In contrast to mammals, which have four Rab3 and two Rab27 genes, *C.*

elegans has only single *rab-3* and *rab-27* genes. Hence, in this study, we used *C. elegans* as a model system to study the requirements for RAB-3 and RAB-27 and their effectors in DCV exocytosis.

Our data suggest that RAB-3 is dispensable for DCV exocytosis in *C. elegans*. We have demonstrated that the release of ectopically expressed neuropeptides, ANF-GFP, was unaffected by the absence of RAB-3 (Figure 1). Our TIRFM experiments also showed that neither the number of DCVs in the TIRF zone nor the dwelling/docking behavior was changed in *rab-3* mutants (Appendix Figure 1). This conclusion is, however, in contrast to a recent study performed with knockout mice. By knocking out the four Rab3 paralogs, the authors proposed that Rab3 proteins play two distinct stimulating roles for DCV exocytosis in embryonic chromaffin cells: (i) facilitating vesicle biogenesis and (ii) stabilizing the primed vesicle state [12]. The rationale behind this discrepancy is unclear. One possibility is that the requirement for Rab proteins may have been finely tuned during evolution. Accordingly, higher organisms may have evolved a design with higher redundancy for the stability of this vital system.

Our data also demonstrated an essential role for RAB-27 in DCV exocytosis in *C. elegans*. Rab27 has been established as a principal docking factor for DCVs in mammals [33,34]. Our TIRF imaging data revealed a role for RAB-27/AEX-6 in the initial attachment/tethering of DCVs to the plasma membrane (Figure 4). This result is consistent with the current model of RAB-27 function and further validates our analysis of DCV docking behavior with TIRFM. We found that RBF-1 is required for both the short-retained DCVs and the long-retained DCVs at the plasma membrane (Figure 4D). Moreover, RAB-27 and RBF-1 act together in the translocation of DCVs to the plasma membrane (Figure 4A). There are some differences in the ANF-GFP release experiments and the TIRFM experiments. In the ANF-GFP release experiments, we used the entire organism as our research subject, and observed the accumulation of ANF-GFP in the coelomocytes and it is also affects by other factors in addition to exocytosis. In contrast, in the TIRFM experiments the object was a *C. elegans* neuron, and RBF-1 was found to be involved in DCVs stabilized docking and its mutant reduced the long-retained events. Based on these results, we propose sequential processes as follows: (i) RAB-27/AEX-6 residing on the DCVs initially recruits rabphilin/RBF-1 for the movement of DCVs along the cytoskeleton network. Moreover, it has been shown that rabphilin facilitates DCV localization within F-actin-rich regions [35]. (ii) Upon approaching the plasma membrane, RAB-27/AEX-6 initiates the tethering/docking process in a dynamic (either sequential or parallel) interaction with proteins, such as rabphilin/RBF-1, SNAP-25 [36], syntaxin and Munc18 [37]. This tethering step is not stable; the vesicles can either return to the cytosol, or proceed to a stabilized docking state. (iii) After the initial tethering step, rabphilin/RBF-1 is further required to stabilize docking and makes DCV fusion competent, with proteins such as (M)unc-13 [38] and SNARE proteins [39]. In depth further investigations on Rabs and their effectors will help characterize the chain of events in the docking and priming of DCVs.

We thank Michael Krause for the KM246 strain and the (p)ida-1::IDA-1::GFP plasmid; Thomas F. J. Martin for the EG3680 strain and the (p)aex-3::ANF::GFP plasmid; and the Caenorhabditis Genetic Center for the other strains. This work was supported by the National Basic Research Program of China (Grant No. 2010CB833701), the National Natural Science Foundation of China (Grant Nos. 30870564 and 90913022), and the CAS Project (Grant No. KSCX2-SW-224).

1 Grosshans B, Ortiz D, Novick P. Rabs and their effectors: achieving specificity in membrane traffic. Proc Natl Acad Sci USA, 2006, 103: 11821–11827
2 Stenmark H. Rab GTPases as coordinators of vesicle traffic. Nat Rev Mol Cell Biol, 2009, 10: 513–525
3 Zerial M, McBride H. Rab proteins as membrane organizers. Nat Rev Mol Cell Biol, 2001, 2: 107–117
4 Fischer von Mollard G, Mignery G A, Baumert M, *et al*. Rab3 is a small GTP-binding protein exclusively localized to synaptic vesicles. Proc Natl Acad Sci USA, 1990, 87: 1988–1992
5 Mahoney T R, Liu Q, Itoh T, *et al*. Regulation of synaptic transmission by RAB-3 and RAB-27 in *Caenorhabditis elegans*. Mol Biol Cell, 2006, 17: 2617–2625
6 Schluter O M, Schmitz F, Jahn R, *et al*. A complete genetic analysis of neuronal Rab3 function. J Neurosci, 2004, 24: 6629–6637
7 Nonet M L, Staunton J E, Kilgard M P, *et al*. *Caenorhabditis elegans* rab-3 mutant synapses exhibit impaired function and are partially depleted of vesicles. J Neurosci, 1997, 17: 8061–8073
8 Johnson J L, Brzezinska A A, Tolmachova T, *et al*. Rab27a and Rab27b regulate neutrophil azurophilic granule exocytosis and NADPH oxidase activity by independent mechanisms. Traffic, 2010, 11: 533–547
9 Gomi H, Mori K, Itohara S, *et al*. Rab27b is expressed in a wide range of exocytic cells and involved in the delivery of secretory granules near the plasma membrane. Mol Biol Cell, 2007, 18: 4377–4386
10 Thiagarajan R, Tewolde T, Li Y, *et al*. Rab3A negatively regulates activity-dependent modulation of exocytosis in bovine adrenal chromaffin cells. J Physiol, 2004, 555: 439–457
11 Chung S H, Joberty G, Gelino E A, *et al*. Comparison of the effects on secretion in chromaffin and PC12 cells of Rab3 family members and mutants. Evidence that inhibitory effects are independent of direct interaction with Rabphilin3. J Biol Chem, 1999, 274: 18113–18120
12 Schonn J S, van Weering J R, Mohrmann R, *et al*. Rab3 proteins involved in vesicle biogenesis and priming in embryonic mouse chromaffin cells. Traffic, 2010, 11: 1415–1428
13 Gonzalez L Jr., Scheller R H. Regulation of membrane trafficking: structural insights from a Rab/effector complex. Cell, 1999, 96: 755–758
14 Stahl B, Chou J H, Li C, *et al*. Rab3 reversibly recruits rabphilin to synaptic vesicles by a mechanism analogous to raf recruitment by ras. EMBO J, 1996,15: 1799–1809
15 Fukuda M, Kanno E, Yamamoto A. Rabphilin and Noc2 are recruited to dense-core vesicles through specific interaction with Rab27A in PC12 cells. J Biol Chem, 2004, 279: 13065–13075
16 Fukuda M. Distinct Rab binding specificity of Rim1, Rim2, rabphilin, and Noc2. Identification of a critical determinant of Rab3A/Rab27A recognition by Rim2. J Biol Chem, 2003, 278: 15373–15380
17 Staunton J, Ganetzky B, Nonet M L. Rabphilin potentiates soluble N-ethylmaleimide sensitive factor attachment protein receptor func-

tion independently of rab3. J Neurosci, 2001, 21: 9255–9264
18 Brenner S. The genetics of Caenorhabditis elegans. Genetics, 1974, 77: 71–94
19 Stiernagle T. Maintenance of *C. elegans*. WormBook, 2006, 1–11
20 Speese S, Petrie M, Schuske K, *et al*. UNC-31 (CAPS) is required for dense-core vesicle but not synaptic vesicle exocytosis in *Caenorhabditis elegans*. J Neurosci, 2007, 27: 6150–6162
21 Christensen M, Estevez A, Yin X, *et al*. A primary culture system for functional analysis of C. elegans neurons and muscle cells. Neuron, 2002, 33: 503–514
22 Strange K, Christensen M, Morrison R. Primary culture of *Caenorhabditis elegans* developing embryo cells for electrophysiological, cell biological and molecular studies. Nat Protoc, 2007, 2: 1003–1012
23 Bai L, Zhu D, Zhou K, *et al*. Differential properties of GTP- and Ca^{2+}-stimulated exocytosis from large dense core vesicles. Traffic, 2006, 7: 416–428
24 Olivo-Marin J C. Extraction of spots in biological images using multiscale products. Pattern Recogn, 2002, 35: 1989–1996
25 Jaqaman K, Loerke D, Mettlen M, *et al*. Robust single-particle tracking in live-cell time-lapse sequences. Nat Methods, 2008, 5: 695–702
26 Weimer R M, Richmond J E, Davis W S, *et al*. Defects in synaptic vesicle docking in unc-18 mutants. Nat Neurosci, 2003, 6: 1023–1030
27 Hata Y, Slaughter C A, Sudhof T C. Synaptic vesicle fusion complex contains unc-18 homologue bound to syntaxin. Nature, 1993, 366: 347–351
28 Oh E, Spurlin B A, Pessin J E, *et al.* Munc18c heterozygous knockout mice display increased susceptibility for severe glucose intolerance. Diabetes, 2005, 54: 638–647
29 Toonen R F, Kochubey O, de Wit H, *et al*. Dissecting docking and tethering of secretory vesicles at the target membrane. EMBO J, 2006, 25: 3725–3737
30 Gordon D E, Bond L M, Sahlender D A, *et al*. A targeted siRNA screen to identify SNAREs required for constitutive secretion in mammalian cells. Traffic, 2010, 11: 1191–1204
31 Zhou K M, Dong Y M, Ge Q, *et al*. PKA activation bypasses the requirement for UNC-31 in the docking of dense core vesicles from *C. elegans* neurons. Neuron, 2007, 56: 657–669
32 Ciufo L F, Barclay J W, Burgoyne R D, *et al*. Munc18-1 regulates early and late stages of exocytosis via syntaxin-independent protein interactions. Mol Biol Cell, 2005, 16: 470–482
33 Fukuda M. Rab27 and its effectors in secretory granule exocytosis: a novel docking machinery composed of a Rab27.effector complex. Biochem Soc Trans, 2006, 34: 691–695
34 Ostrowski M, Carmo N B, Krumeich S, *et al*. Rab27a and Rab27b control different steps of the exosome secretion pathway. Nat Cell Biol, 2010, 12: 19-30; sup 11–13
35 Baldini G, Martelli A M, Tabellini G, *et al*. Rabphilin localizes with the cell actin cytoskeleton and stimulates association of granules with F-actin cross-linked by {alpha}-actinin. J Biol Chem, 2005, 280: 34974–34984
36 Tsuboi T, Fukuda M. The C2B domain of rabphilin directly interacts with SNAP-25 and regulates the docking step of dense core vesicle exocytosis in PC12 cells. J Biol Chem, 2005, 280: 39253–39259
37 Tsuboi T. Molecular mechanism of attachment process of dense-core vesicles to the plasma membrane in neuroendocrine cells. Neurosci Res, 2009, 63: 83–88
38 Deng L, Kaeser P S, Xu W, *et al*. RIM proteins activate vesicle priming by reversing autoinhibitory homodimerization of Munc13. Neuron, 2011, 69: 317–331
39 Xu T, Rammner B, Margittai M, *et al*. Inhibition of SNARE complex assembly differentially affects kinetic components of exocytosis. Cell, 1999, 99: 713–722

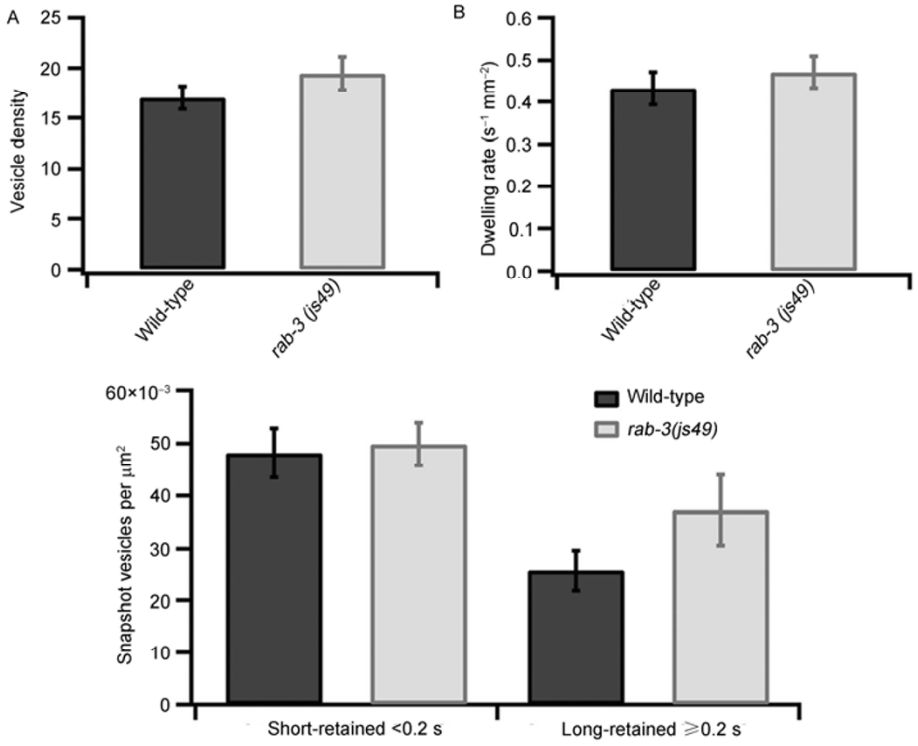

Appendix Figure 1 Investigating the role of RAB-3 in DCV secretion by TIRFM. A, Density of visible DCVs in the evanescent field in wild-type and *rab-3(js49)* mutants. B, Dwelling rate of DCVs (per second per unit area) in wide-type (n=16) and *rab-3(js49)* (n=12) mutants. C, Averaged vesicle abundance at given times during image acquisition grouped according to their residency times at the membrane.